

7. G. S. Bays and W. S. McAdams, *Ind. Eng. Chem.*, **29**, No. 11 (1937).
8. W. Nusselt, *Z. VDI*, **67**, No. 9 (1923).
9. J. A. Prins, J. Mulder, and J. Shenk, *Appl. Sci. Res.*, **A2**, 431 (1950).
10. V. I. Kholostykh, Author's Abstract of Candidate's Dissertation, Ural Polytechnic Institute, Sverdlovsk (1971).
11. K. R. Das, Author's Abstract of Candidate's Dissertation, Kiev Polytechnic Institute (1971).

NATURAL CONVECTIVE HEAT EXCHANGE BETWEEN ISOTHERMAL CONCENTRIC SPHERES

S. V. Solov'ev and A. S. Lyalikov

UDC 536.25

The problem of natural convection in spherically concentric layers is considered. The heat-exchange similarity equation obtained agrees satisfactorily with the experimental data of [5].

At the present time there is great interest in analytical and numerical methods of solving natural convective problems in finite volumes. The majority of studies consider planar problems, with a minority devoted to cylindrical layers, while [1-3] consider spherical layers. A bibliography of the first two types of problem is presented in [4]. In [1] the authors consider natural convection of a viscous compressible gas (air, $P = 0.714$) for outer/inner diameter ratios in the range $1.1 \leq d_2/d_1 \leq 6$ and Grashof numbers from 10^3 to 10^6 . Lawrence et al. [2] considered natural convection of incompressible air at low Rayleigh numbers. The authors attempted to fill a gap in theory for this region, but comparison of their results with the experiments of Bishop et al. [5] indicates a lack of success. In [3] (where in contrast to [1, 2] the exterior sphere was the hotter), natural convection of a compressible gas (air, $P = 0.71$) was considered. The heat-exchange similarity equation obtained in [3] was compared with the results of [5] and good agreement was found.

In the experimental study [5] a generalized heat-exchange equation was obtained for calculation of average heat liberation in spherical isothermal concentric layers for a wide range of Rayleigh numbers (determined by width of the layer) and Prandtl numbers ($P = 4.7-4148$; $Ra = 1.3 \cdot 10^3-5.8 \cdot 10^6$, $D/d = 1.09-2.81$).

But, it is often of importance to know such local characteristics as the velocity field, the temperature in the layer, the character of liquid motion, and local thermal fluxes (which are often quite complex), which at present cannot be experimentally determined. These difficulties may be avoided by numerical solution of the problem. Moreover, [1-3] considered only air, reducing the range of application of the analytical and numerical results obtained for calculation of natural convective heat exchange in spherical concentric liquid (gas) layers, the thermophysical characteristics of which differ from air. Therefore, in order to obtain a solution over a broadened range of Prandtl and Rayleigh numbers, an attempt was made to numerically solve the problem of natural convection in spherical concentric layers of both gases and liquids. Prandtl and Rayleigh numbers were varied over the range $P = 0.2-5$, $Ra_d =$

TABLE 1. Coefficients of Eq. (1)

φ	a_φ	b_φ	c_φ	d_φ
$\frac{\omega}{R \sin \beta}$	$\frac{R^2 \sin^2 \beta}{GP^2}$	$\frac{R^2 \sin^2 \beta}{GP}$	1	$R \sin \beta \left(\sin \beta \frac{\partial T}{\partial R} + \frac{\cos \beta}{R} \frac{\partial T}{\partial \beta} \right)$
ψ	0	$\frac{1}{R^2 \sin^2 \beta}$	1	$-\frac{\omega}{R^2 \sin^2 \beta}$
T	1	1	1	0

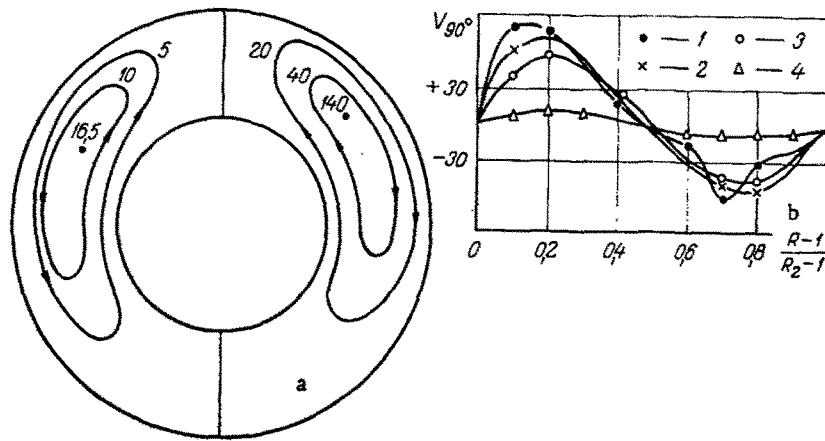


Fig. 1. Flow line distribution for spherical layer with $d/D = 0.5$, $P = 1$, $G = 10^4$ (left) and $P = 1.25$, $G = 10^5$ (right) (a); tangential velocity component at $\beta = 90^\circ$ for various d/D ($P = 3.96$, $Ra_d = 3.16 \cdot 10^5$) (b): 1) $d/D = 0.5$; 2) 0.59; 3) 0.67; 4) 0.83.

$8 \cdot (10^3 - 10^7)$. Inner/outer diameter ratio of the spheres was varied over the range $0.5 \leq d/D \leq 0.83$.

The stationary problem of motion and heat exchange upon natural convection in spherical concentric layers with a heated inner sphere was considered. The problem was described by the Navier-Stokes equation and the equations of continuity and energy conservation in the Boussinesq approximation with consideration of longitudinal symmetry. Solution reduces to solution of three equations: for eddy-current intensity, energy, and the Poisson equation for the current function. In dimensionless form these equations may be combined in the form

$$a_\varphi \left\{ \frac{\partial}{\partial R} \left(\varphi \frac{\partial \psi}{\partial \beta} \right) - \frac{\partial}{\partial \beta} \left(\varphi \frac{\partial \psi}{\partial R} \right) \right\} - \frac{\partial}{\partial R} \left\{ b_\varphi R^2 \sin \beta \frac{\partial (C_\varphi \psi)}{\partial R} \right\} - \frac{\partial}{\partial \beta} \left\{ b_\varphi \sin \beta \frac{\partial (C_\varphi \psi)}{\partial \beta} \right\} + R^2 d_\varphi \sin \beta = 0. \quad (1)$$

The coefficients φ , a_φ , b_φ , c_φ , d_φ are defined in Table 1.

The boundary conditions which must be satisfied by the solution of Eq. (1) are:

$$\psi = \frac{\partial \psi}{\partial R} = 0 \quad \text{at } R = 1, R_2, \quad (2)$$

where

$$\psi = \frac{\partial^2 \psi}{\partial \beta^2} = \frac{\partial T}{\partial \beta} = 0 \quad \text{at } \beta = 0, \pi, \quad (3)$$

$$T = 1 \quad \text{at } R = 1, \quad (4)$$

$$T = 0 \quad \text{at } R = R_2. \quad (5)$$

The boundary conditions for vortex intensity on the wall assume a linear change of ω along the normal. The boundary condition for ω on the axis of symmetry is taken from [6]. As scales for the radius, flow function, and temperature, we use r_1 , the thermal diffusivity α , and $t_1 - t_2$, respectively.

Equation (1) was solved by the method described in [6]. For the initial values of the desired functions the zero values of vortex intensity, flow function, and stationary temperature distribution T_* for the case of pure thermal conductivity [2] were used:

$$T_* = \frac{R_2 - R}{R(R_2 - 1)}. \quad (6)$$

Calculations were performed on a grid with 10-20 steps in radius and 30-36 steps in angle.

Stationary flow line distribution, tangential velocity component, temperature, and local Nusselt number were obtained.

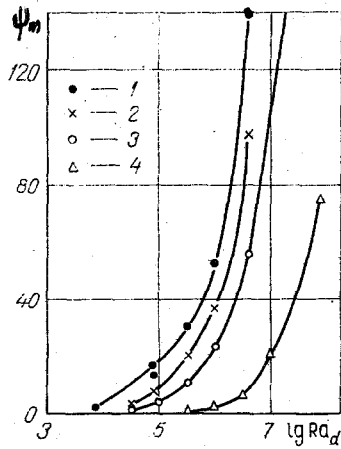


Fig. 2. Maximum of flow function ψ_m versus log of Rayleigh number for various d/D . For experimental-point notation see Fig. 1.

Figure 1a shows flow lines for $d/D = 0.5$, $P = 1$, $G = 10^4$ (left) and $P = 1.25$, $G = 10^5$ (right). With increase in Reynolds number there is an increase in flow function values. In these regimes there is a single vortex flow, with the center of the vortex (denoted by a dot) displaced upward.

Figure 1b shows that the velocity profiles $V_{\theta,0^\circ}$ for various d/D ($P = 3.96$, $Ra_d = 3.16 \cdot 10^5$) are of identical character, with the exception of the profile for $d/D = 0.5$ in the region next to the outer surface, which is explained by the existence of a secondary vortex in this region.

As shown in Fig. 2, the maximum of the flow function ψ_m as a function of $\lg Ra_d$ for various d/D always increases monotonically with increase in Rayleigh number. (For $d/D = 0.67$ the flow function maximum increases to $\psi_m = 189$, which corresponds to a value $Ra_d = 4 \cdot 10^7$, where $d = 2r_1$.)

Figure 3 shows temperature profiles for $P = 3.96$, $Ra_d = 3.16 \cdot 10^5$, and various d/D . As is apparent from the figure, with decrease in d/D (i.e., upon increase in the width of the layer) there occurs a certain readjustment of the temperature field, in the sense that with increase in β there is an increase in temperature gradients on the surface of the inner sphere with relative lack of change on the surface of the outer sphere, which agreed qualitatively with the velocity profiles of Fig. 1b and the experimental temperature profiles of [5].

Figure 4a shows local Nusselt numbers on the surfaces of inner and outer spheres

$$Nu_1 = \frac{\alpha_1 r_1}{\lambda} = - \left. \frac{\partial T}{\partial R} \right|_{R=1}, \quad (7)$$

$$Nu_2 = \frac{\alpha_2 r_2}{\lambda} = - R_2 \left. \frac{\partial T}{\partial R} \right|_{R=R_2}, \quad (8)$$

with the derivatives of Eqs. (7), (8) approximated by three-point formulas:

$$\frac{1}{2\Delta R} (4T_1 - 3T_0 - T_2) \text{ and } \frac{1}{2\Delta R} (T_{N-2} + 3T_N - 4T_{N-1}).$$

Nusselt numbers were averaged over the surfaces $R = 1$ and $R = R_2$ in the form

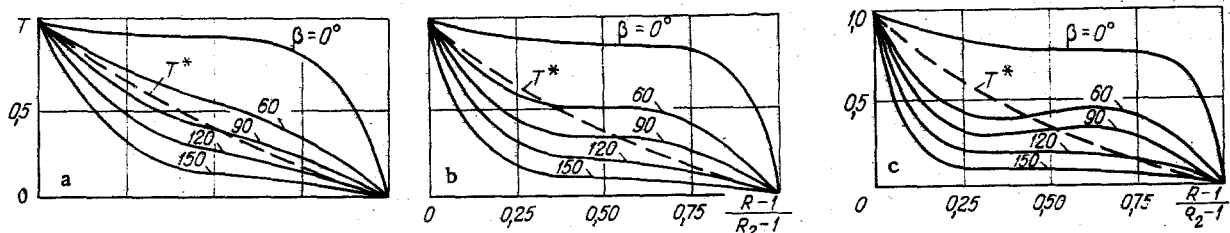


Fig. 3. Temperature distribution T_* in layer at various angles β . $P = 3.96$, $Ra_d = 3.16 \cdot 10^5$; * a) $d/D = 0.67$; b) 0.59 ; c) 0.5 .

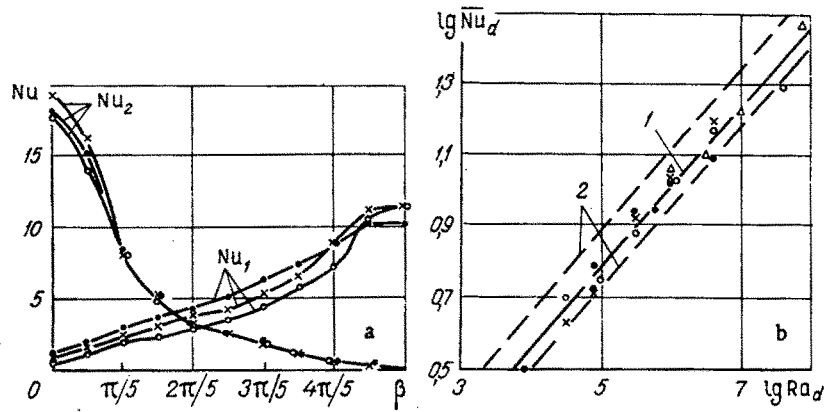


Fig. 4. Distribution of local Nusselt numbers on inner (Nu_1) and outer (Nu_2) spheres for various angles β ($P = 3.96$, $Ra_d = 3.16 \cdot 10^3$) (a), and comparison of Eq. (12) derived herein with generalized experimental data of Eq. (14) (b): 1) Eq. (12); 2) Eq. (14).

$$\bar{Nu}_{r_1} = \frac{\bar{\alpha}_1 r_1}{\lambda} = -\frac{1}{2} \int_0^\pi \left[\frac{\partial T}{\partial R} \right]_{R=r_1} \sin \beta d\beta, \quad (9)$$

$$\bar{Nu}_{r_2} = \frac{\bar{\alpha}_2 r_2}{\lambda} = -\frac{R_2}{2} \int_0^\pi \left[\frac{\partial T}{\partial R} \right]_{R=R_2} \sin \beta d\beta.$$

Verification with the balance equation

$$\bar{\alpha}_1 \Delta t 4\pi r_1^2 = \bar{\alpha}_2 \Delta t 4\pi r_2^2 \quad (10)$$

showed that the curves of Fig. 4a satisfy Eq. (10).

As is evident from Fig. 4a, the local Nusselt numbers depend weakly on d/D , the same conclusion reached by the authors of [3].

To obtain a heat-exchange similarity equation for free convection in spherical layers, the averaged Nusselt number \bar{Nu}_{r_1} was calculated in accordance with Eq. (9) for 22 variants of original data. The integral in Eq. (9) was calculated by Simpson's rule.

Figure 4b shows the dependence of averaged Nusselt numbers on Rayleigh number (referred to the diameter of the inner sphere). These data were processed by the least-squares method [7], with data approximated by the expression

$$\bar{Nu}_d = a_0 (d/D)^{a_1} Ra_d^{a_2}, \quad (11)$$

where a_0 , a_1 , a_2 are unknown coefficients.

The least-squares method was also used to obtain the expression

$$\bar{Nu}_d = 0.450 (d/D)^{0.031} Ra_d^{0.226}, \quad (12)$$

which is evaluated statistically in Table 2.

From Eq. (12) it is evident that the averaged Nusselt number does in fact depend weakly on d/D . The equation thus obtained, Eq. (12), was compared with the generalized experimental

TABLE 2. Statistical Evaluation of Coefficients of Eq. (11)

Quantity	σ	w
$a_0 = 0.450$	0.071	0.287
$a_1 = 0.031$	0.120	0.100
$a_2 = 0.226$	0.009	16.449

$$\sigma_0 = 0.038; S = 0.029$$

data of [5]:

$$k_{\text{eff}}/k = 0,228 (Ra^*)^{0,226}, \quad (13)$$

which when transformed to Nusselt number and inner sphere diameter as defining dimension takes on the form

$$\overline{Nu}_d = (0,572 - 0,394) Ra_d^{0,226}. \quad (14)$$

The change in the constant within parentheses is related to the range of change of d/D , while the constant of Eq. (12) lies within this interval with a relative error of -21% to $+14\%$.

Thus, the similarity equation obtained, Eq. (12), satisfactorily describes natural convection in spherical concentric layers with the heat exchange regimes considered, permitting evaluation of the probability (reliability) of local values obtained, a knowledge of which is necessary for calculation of a given phenomenon.

NOTATION

r_1, r_2 , dimensional radii of inner and outer spheres; d, D , dimensional diameters of inner and outer spheres; t_1 and t_2 , temperatures on inner and outer sphere surfaces; T_* , stationary temperature distribution in case of pure thermal conductivity; R and R_2 , dimensionless current radius and radius of outer sphere, ψ , flow function; ω , vortex intensity; β , polar angle; $P = \nu/a$, Prandtl number; $Ra_d = g\gamma(t_1 - t_2)d^3/(\nu a)$, Rayleigh number; $G = g\gamma(t_1 - t_2)r_1^3/\nu^2$, Grashof number; T , dimensionless temperature; γ , coefficient of thermal expansion; $Nu_1 = \alpha_1 r_1/\lambda$ and $Nu_2 = \alpha_2 r_2/\lambda$, local Nusselt numbers on inner and outer surfaces; $Nu_{r_1} = \overline{\alpha}_1 r_1/\lambda$ and $Nu_{r_2} = \overline{\alpha}_2 r_2/\lambda$, averaged Nusselt numbers on inner and outer sphere surfaces; α_1 and α_2 , local heat liberation coefficients on inner and outer surfaces; $\overline{\alpha}_1$ and $\overline{\alpha}_2$, averaged heat liberation coefficients on inner and outer surfaces; λ , thermal conductivity coefficient of liquid; $Nu_d = \overline{\alpha}_1 d/\lambda$, averaged Nusselt number on inner sphere surface; k_{eff} and k , effective and molecular thermal conductivity coefficients; a , thermal diffusivity coefficient; $Re^* = g\gamma\Delta T(r_o - r_1)^4/\nu a r_1$, modified Rayleigh number; r_o, r_1 , radii of inner and outer spheres; $V_{\theta, \beta}$, tangential velocity component at $\beta = 90^\circ$; σ , mean-square error; w , weight function; σ_o , mean-square error per unit weight; S , residual quadratic function.

LITERATURE CITED

1. S. I. Al'ber and N. M. Stankevich, "Heat exchange upon natural convection in spherical layers," in: Second All-Union Conference on Contemporary Problems of Thermal Convection, Summaries of Reports [in Russian], Perm (1975).
2. R. Mark Lawrence and Harry C. Hardee, "Natural convection between concentric spheres at low Rayleigh numbers," *Int. J. Heat Mass Transfer*, 11, 387 (1968).
3. G. B. Petrazhitskii and N. M. Stankevich, "Natural convection of a compressible liquid in spherical layers," *Zh. Prik. Mekh. Tekh. Fiz.*, No. 5 (1976).
4. A. V. Lykov and B. M. Berkovskii, *Convection and Thermal Waves* [in Russian], Énergiya, Moscow (1974).
5. J. A. Scanlan, E. H. Bishop, and R. E. Powe, "Natural convection heat transfer between concentric spheres," *Int. J. Heat Mass Transfer*, 13, 1857 (1970).
6. A. D. Gosman, V. M. Pan, A. K. Ranchel, D. B. Spaulding, and M. Wolfstein, *Numerical Methods in the Study of Flows of Viscous Liquid* [Russian translation], Mir, Moscow (1972).
7. R. S. Guter and B. V. Ovchinskii, *Elements of Numerical Analysis and Mathematical Processing of Experimental Data* [in Russian], 2nd ed., Nauka, Moscow (1970).